Supporting Information

Covalent and Non-covalent Conjugation of Few-Layered Graphene Oxide and Ruthenium(II) Complex Hybrids and Their Energy Transfer Modulation Via Enzymatic Hydrolysis

Frankie Chi-Ming Leung [a] and Vivian Wing-Wah Yam [a]*

[a] Institute of Molecular Functional Materials (Areas of Excellence Scheme, University Grants Committee (Hong Kong)) and Department of Chemistry, The University of Hong Kong, Pokfulam Road, Hong Kong SAR, P. R. China

E-mail: wwyam@hku.hk

Experimental Section

Materials and Reagents.

4-Methyl-4'-carboxy-2,2'-bipyridine (bpy-COOH),[1] 1-pyrenemethanol (pyr-OH),[2] pyrene-CH_2-(OC_2H_4)-OH (pyr-EO1),[3] pyrene-CH_2-$(OC_2H_4)_2$-OH (pyr-EO2),[3] pyrene-CH_2-$(OC_2H_4)_3$-OH (pyr-EO3),[3] pyrene-CH_2-$(OC_2H_4)_4$-OH (pyr-EO4),[3] 1-(pyren-1-yl)-2,5,8,11-tetraoxatridecan-13-ammonium bromide (pyr-NMe_3^+),[4] $[Ru(bpy)_2(bpy\text{-}CH_2OH)]Cl_2$,[5] $[Ru(bpy)_2(bpy\text{-}COOMe)]Cl_2$,[5] *cis*-$[Ru(bpy)_2Cl_2]$[5] and $[Re(CO)_5Br]$[6] were synthesized according to the literature methods. Graphite flakes, hydrazine monohydrate, 4-formylbenzoic acid, sarcosine, hydroxybenzotriazole (HOBt), potassium persulfate ($K_2S_2O_8$), potassium permanganate ($KMnO_4$), porcine liver esterase (PLE) suspension in $(NH_4)_2SO_4$ (3.2 M, pH 8.0) (≥150 units/mg protein (biuret)) were purchased from Sigma-Aldrich. One unit of esterase will hydrolyze 1.0 μmole of ethyl butyrate to butyric acid and ethanol per min at pH 8.0 at 25 °C. Scheme S1 shows the synthetic pathway for the target ligands and complexes.

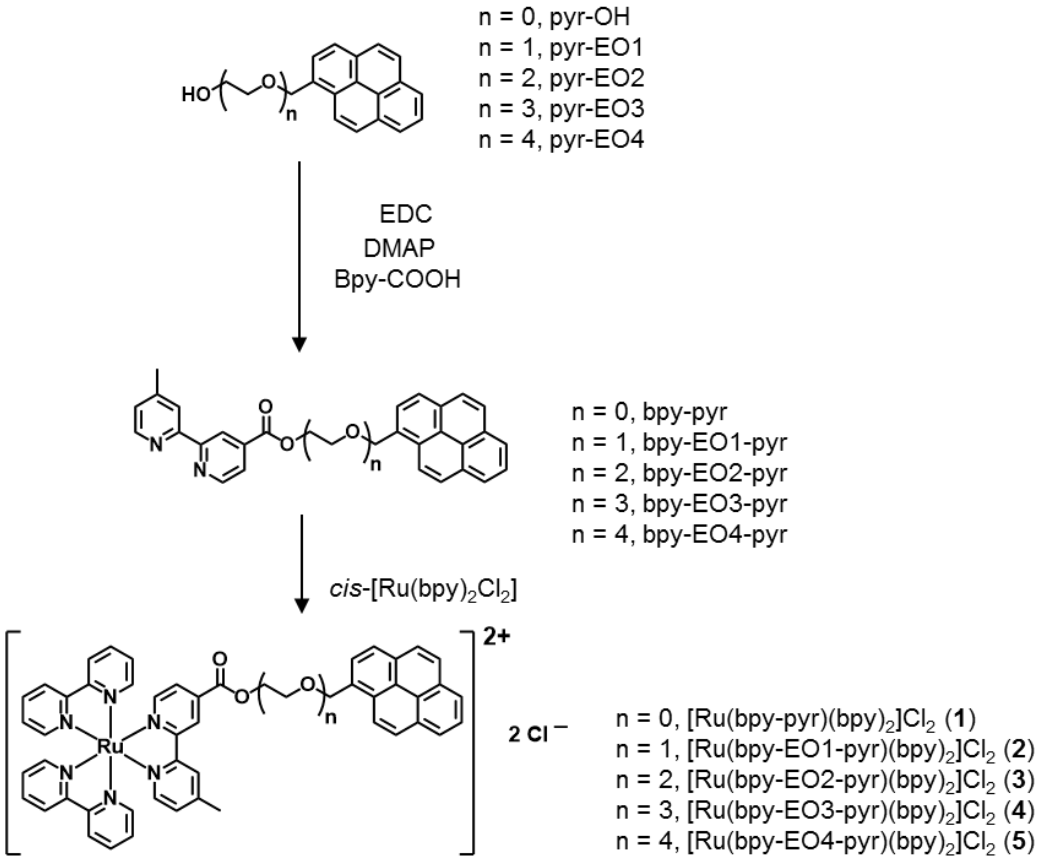

Scheme S1. Synthetic routes for complexes **1**–**5**.

Synthesis of bpy-pyr

The ligand bpy-pyr was synthesized according to the modification of a literature procedure reported for esterification.[7] 4-Methyl-4'-carboxy-2,2'-bipyridine (bpy-COOH, 0.54 g, 2.5 mmol), pyr-OH (0.6 g, 2.6 mmol), EDC•HCl (0.50 g, 2.6 mmol) and DMAP (0.32 g, 2.6 mmol) were dissolved in dry CH_2Cl_2 (20 mL) and stirred at room temperature for overnight under an inert atmosphere of nitrogen. The solvent was removed in vacuo, and then the residue was column chromatographed on silca gel with $CHCl_3$ as the eluent to give the desired ligand as a colorless liquid. Yield: 0.9 g (85 %). Positive EI-MS: ion clusters at m/z 428 $[M]^+$. ^{1}H NMR (400 MHz, $CDCl_3$, 298 K, relative to Me_4Si, δ / ppm): δ = 2.43 (s, 3H, $–CH_3$), 6.16 (s, 2H, pyr$–CH_2O–$), 7.14 (d, *J* = 5.2 Hz, 1H, bpy), 7.86 (dd, *J* = 5.2, 1.2 Hz, 1H, bpy), 8.00–8.26 (m, 9H, pyr + bpy), 8.41 (d, *J* = 9.2 Hz, 1H, pyr), 8.52 (d, *J* = 5.2 Hz, 1H, bpy), 8.77 (d, *J* = 5.2 Hz, 1H, bpy), 8.94 (s, 1H, bpy). IR (KBr) *ν* / cm^{-1}: 2936 (m, sh, *ν*($–CH_3$)), 1762 (s, sh, *ν*(C=O)), 1143 (s, sh, *ν*(C–O)).

Synthesis of bpy-EO1-pyr

The procedure was similar to that described for the synthesis of bpy-pyr, except pyr-EO1 (0.72 g, 2.6 mmol) was used instead of pyr-OH to give the desired ligand as a white solid. Yield: 944 mg (80 %). Positive EI-MS: ion clusters at m/z 472 $[M]^+$. ^{1}H NMR (400 MHz, $CDCl_3$, 298 K, relative to Me_4Si, δ / ppm): δ = 2.44 (s, 3H, $–CH_3$), 4.01–4.09 (m, 2H, $–OCH_2–$), 4.58–4.67 (m, 2H, $–OCH_2–$), 5.48 (s, 2H, pyr$–CH_2O–$), 7.16 (d, *J* = 5.2Hz, 1H, bpy), 7.87 (d, *J* = 5.2 Hz, 1H, bpy), 7.99–8.28 (m, 9H, pyr + bpy), 8.42 (d, *J* = 9.2 Hz, 1H, pyr), 8.56 (d, *J* = 5.2 Hz, 1H, bpy), 8.80 (d, *J* = 5.2 Hz, 1H, bpy), 8.94 (s, 1H, bpy). IR (KBr) *ν* / cm^{-1}: 2933 (m, sh, *ν*($–CH_3$)), 1764 (s, sh, *ν*(C=O)), 1152 (s, sh, *ν*(C–O)).

Synthesis of bpy-EO2-pyr

The procedure was similar to that described for the synthesis of bpy-pyr, except pyr-EO2 (0.83 g, 2.6 mmol) was used instead of pyr-OH to give the desired ligand as a white solid. Yield: 942 mg (73 %). Positive EI-MS: ion clusters at m/z 516 $[M]^+$. ^1H NMR (300 MHz, $CDCl_3$, 298 K, relative to Me_4Si, δ / ppm): δ = 2.46 (s, 3H, $–CH_3$), 3.80 (s, 4H, $–OCH_2–$), 3.87–3.93 (m, 2H, $–OCH_2–$), 4.54–4.59 (m, 2H, $–OCH_2–$), 5.38 (s, 2H, pyr$–CH_2O–$), 7.18 (d, *J* = 5.4 Hz, 1H, bpy), 7.87 (d, *J* = 5.4 Hz, 1H, bpy), 7.97–8.30 (m, 9H, pyr + bpy), 8.41 (d, *J* = 9.2 Hz, 1H, pyr), 8.60 (d, *J* = 5.4 Hz, 1H, bpy), 8.84 (d, *J* = 5.4 Hz, 1H, bpy), 8.95 (s, 1H, bpy). IR (KBr) *v* / cm^{-1}: 2939 (m, sh, *v*($–CH_3$)), 1755 (s, sh, *v*(C=O)), 1142 (s, sh, *v*(C–O)).

Synthesis of bpy-EO3-pyr

The procedure was similar to that described for the synthesis of bpy-pyr, except pyr-EO3 (0.95 g, 2.6 mmol) was used instead of pyr-OH to give the desired ligand as a white solid. Yield: 1.08 g (77 %). Positive EI-MS: ion clusters at m/z 560 $[M]^+$. ^1H NMR (400 MHz, $CDCl_3$, 298 K, relative to Me_4Si, δ / ppm): δ = 2.43 (s, 3H, $–CH_3$), 3.66–3.79 (m, 6H, $–OCH_2–$), 3.79–3.85 (m, 2H, $–OCH_2–$), 3.85–3.90 (m, 2H, $–OCH_2–$), 4.47–4.53 (m, 2H, $–OCH_2–$), 5.32 (s, 2H, pyr$–CH_2O–$), 7.16 (d, *J* = 5.6 Hz, 1H, bpy), 7.84 (d, *J* = 5.6 Hz, 1H, bpy), 7.97–8.25 (m, 9H, pyr + bpy), 8.40 (d, *J* = 9.2 Hz, 1H, pyr), 8.60 (d, *J* = 5.6 Hz, 1H, bpy), 8.80 (d, *J* = 5.6 Hz, 1H, bpy), 8.93 (s, 1H, bpy). IR (KBr) *v* / cm^{-1}: 2932 (m, sh, *v*($–CH_3$)), 1747 (s, sh, *v*(C=O)), 1175 (m, sh, *v*(C–O)).

Synthesis of bpy-EO4-pyr

The procedure was similar to that described for the synthesis of bpy-pyr, except pyr-EO4 (1.06 g, 2.6 mmol) was used instead of pyr-OH to give the desired ligand as a white solid. Yield: 876 mg (58 %). Positive EI-MS: ion clusters at m/z 604 $[M]^+$. ^1H NMR (400 MHz, $CDCl_3$, 298 K, relative to Me_4Si, δ / ppm): δ = 2.43 (s, 3H, $–CH_3$), 3.60–3.72 (m, 10H, $–OCH_2–$), 3.72–3.77 (m, 2H, $–OCH_2–$), 3.77–3.82 (m, 2H, $–OCH_2–$), 4.46–4.51 (m, 2H, $–OCH_2–$), 5.27 (s, 2H, pyr–$CH_2O–$), 7.13 (d, *J* = 4.8 Hz, 1H, bpy), 7.83 (d, *J* = 4.8 Hz, 1H, bpy), 7.97–8.22 (m, 9H, pyr + bpy), 8.39 (d, *J* = 9.2 Hz, 1H, pyr), 8.55 (d, *J* = 4.8 Hz, 1H, bpy), 8.77 (d, *J* = 4.8 Hz, 1H, bpy), 8.90 (s, 1H, bpy). IR (KBr) *v* / cm^{-1}: 2931 (m, sh, *v*($–CH_3$)), 1757 (s, sh, *v*(C=O)), 1173 (s, sh, *v*(C–O)).

Synthesis of $[Ru(bpy\text{-}pyr)(bpy)_2]Cl_2$ (Complex 1)

The complex was synthesized according to the modification of a literature procedure for $[Ru(bpy)_2(N\text{^}N)]Cl_2$.[8] bpy-pyr (116 mg, 0.5 mmol) was added to a solution of *cis*-$[Ru(bpy)_2Cl_2]•2H_2O$ (261 mg, 0.5 mmol) in absolute ethanol (50 mL). The mixture was then refluxed under N_2 for 5 hours. The purple black solution turned red orange. The solvent was removed in vacuum and the residue was washed with diethyl ether to remove the unreacted ligands. The crude product was purified by recrystallization via vapor diffusion of diethyl ether into an acetonitrile solution of the complex to afford the desired complex as a red solid. Yield: 269 mg (59 %). Positive ESI-MS: ion clusters at m/z 877 $[M–Cl]^+$, 421 $[M–2Cl]^{2+}$. ^1H NMR (300 MHz, CD_3CN, 298 K, relative to Me_4Si, δ / ppm): δ = 2.52 (s, 3H, $–CH_3$), 6.2 (s, 2H, pyr–$CH_2O–$), 7.26 (d, *J* = 5.4 Hz, 1H, bpy), 7.29–7.44 (m, 4H, bpy), 7.54 (d, *J* = 5.4, 1H, bpy), 7.62–7.75 (m, 4H, bpy), 7.77 (d, *J* = 5.4 Hz, 1H, bpy), 7.87 (d, *J* = 5.4 Hz, 1H, bpy), 7.97–8.38 (m, 13H, bpy), 8.43–8.59 (m, 5H, bpy + pyr), 8.90 (s, 1H, bpy).

IR (KBr) ν / cm^{-1}: 2936 (m, sh, ν(–CH_3)), 1763 (s, sh, ν(C=O)), 1145 (s, sh, ν(C–O)). Elemental analyses calcd. (%) for $C_{49}H_{36}Cl_2N_6O_2Ru\bullet 2H_2O$: C, 62.02; H, 4.25; N, 8.86. Found: C, 62.22; H, 4.37; N, 8.70.

Synthesis of [Ru(bpy-EO1-pyr)(bpy)$_2$]Cl$_2$ (Complex 2)

The procedure was similar to that described for the synthesis of complex **1**, except bpy-EO1-pyr (138 mg, 0.5 mmol) was used instead of bpy-pyr to give the desired complex as a red solid. Yield: 292 mg (61 %). Positive ESI-MS: ion clusters at m/z 921 $[M–Cl]^+$, 443 $[M–2Cl]^{2+}$. ^{1}H NMR (300 MHz, CD_3CN, 298 K, relative to Me_4Si, δ / ppm): δ = 2.51 (s, 3H, –CH_3), 4.16–4.24 (m, 2H, –OCH_2–), 4.58–4.65 (m, 2H, –OCH_2–), 5.52 (s, 2H, pyr–CH_2O–), 7.25 (d, J = 5.4 Hz, 1H, bpy), 7.27–7.44 (m, 4H, bpy), 7.53 (d, J = 5.4, 1H, bpy), 7.59–7.76 (m, 5H, bpy), 7.86 (d, J = 5.4 Hz, 1H, bpy), 7.95–8.13 (m, 9H, pyr + bpy), 8.16–8.34 (m, 4H, bpy), 8.40 (d, J = 9.3 Hz, 1H, pyr), 8.42–8.56 (m, 4H, bpy), 8.86 (s, 1H, bpy). IR (KBr) ν / cm^{-1}: 2933 (m, sh, ν(–CH_3)), 1765 (s, sh, ν(C=O)), 1151 (s, sh, ν(C–O)). Elemental analyses calcd. (%) for $C_{51}H_{40}Cl_2N_6O_3Ru\bullet H_2O\bullet$MeOH: C, 62.03; H, 4.60; N, 8.35. Found: C, 62.17; H, 4.62; N, 8.44.

Synthesis of [Ru(bpy-EO2-pyr)(bpy)$_2$]Cl$_2$ (Complex 3)

The procedure was similar to that described for the synthesis of complex **1**, except bpy-EO2-pyr (160 mg, 0.5 mmol) was used instead of bpy-pyr to give the desired complex as a red solid. Yield: 250 mg (50 %). Positive ESI-MS: ion clusters at m/z 965 $[M–Cl]^+$, 465 $[M–2Cl]^{2+}$. ^{1}H NMR (300 MHz, CD_3CN, 298 K, relative to Me_4Si, δ / ppm): δ = 2.50 (s, 3H, –CH_3), 3.64–3.71 (m, 4H, –OCH_2–), 3.82–3.90 (m, 2H,

–OCH_2–), 4.46–4.53 (m, 2H, –OCH_2–), 5.32 (s, 2H, pyr–CH_2O–), 7.21–7.43 (m, 5H, bpy), 7.53 (d, *J* = 5.2, 1H, bpy), 7.60–7.73 (m, 5H, bpy), 7.85 (d, *J* = 5.2 Hz, 1H, bpy), 7.93–8.15 (m, 9H, pyr + bpy), 8.18–8.32 (m, 4H, bpy), 8.37 (d, *J* = 9.2 Hz, 1H, pyr), 8.40–8.54 (m, 4H, bpy), 8.83 (s, 1H, bpy). IR (KBr) ν / cm^{-1}: 2937 (m, sh, ν(–CH_3)), 1756 (s, sh, ν(C=O)), 1142 (s, sh, ν(C–O)). Elemental analyses calcd. (%) for $C_{53}H_{44}Cl_2N_6O_4Ru \bullet H_2O$: C, 62.47; H, 4.55; N, 8.25. Found: C, 62.33; H, 4.70; N, 7.97.

Synthesis of [Ru(bpy-EO3-pyr)(bpy)$_2$]Cl$_2$ (Complex 4)

The procedure was similar to that described for the synthesis of complex **1**, except bpy-EO3-pyr (182 mg, 0.5 mmol) was used instead of bpy-pyr to give the desired complex as a red solid. Yield: 287mg (55 %). Positive ESI-MS: ion clusters at m/z 487 $[M–2Cl]^{2+}$. ^{1}H NMR (400 MHz, CD_3CN, 298 K, relative to Me_4Si, δ / ppm): δ = 2.50 (s, 3H, –CH_3), 3.50–3.68 (m, 6H, –OCH_2–), 3.69–3.75 (m, 2H, –OCH_2–), 3.77–3.82 (m, 2H, –OCH_2–), 4.38–4.46 (m, 2H, –OCH_2–), 5.16 (s, 2H, pyr–CH_2O–), 7.18–7.45 (m, 5H, bpy), 7.53 (d, *J* = 5.2, 1H, bpy), 7.59–7.70 (m, 5H, bpy), 7.85 (d, *J* = 5.2 Hz, 1H, bpy), 7.91–8.19 (m, 11H, pyr + bpy), 8.20–8.28 (m, 2H, bpy), 8.35 (d, *J* = 9.2 Hz, 1H, pyr), 8.37–8.53 (m, 4H, bpy), 8.80 (s, 1H, bpy). IR (KBr) ν / cm^{-1}: 2932 (m, sh, ν(–CH_3)), 1745 (s, sh, ν(C=O)), 1176 (m, sh, ν(C–O)). Elemental analyses calcd. (%) for $C_{55}H_{48}Cl_2N_6O_5Ru \bullet 2MeOH$: C, 61.73; H, 5.09; N, 7.58. Found: C, 61.91; H, 5.12; N, 7.49.

Synthesis of [Ru(bpy-EO4-pyr)(bpy)$_2$]Cl$_2$ (Complex 5)

The procedure was similar to that described for the synthesis of complex **1**, except bpy-EO4-pyr (204 mg, 0.5 mmol) was used instead of bpy-pyr to give the desired

complex as a red solid. Yield: 234 mg (43 %). Positive ESI-MS: ion clusters at m/z 509 $[M-2Cl]^{2+}$. ^{1}H NMR (300 MHz, CD_3CN, 298 K, relative to Me_4Si, δ / ppm): δ = 2.52 (s, 3H, $-CH_3$), 3.48–3.62 (m, 10H, $-OCH_2-$), 3.69–3.75 (m, 4H, $-OCH_2-$), 4.34–4.41 (m, 2H, $-OCH_2-$), 5.18 (s, 2H, pyr–CH_2O-), 7.24 (d, *J* = 5.4 Hz, 1H, bpy), 7.27–7.44 (m, 4H, bpy), 7.53 (d, *J* = 5.4, 1H, bpy), 7.58–7.70 (m, 5H, bpy), 7.86 (d, *J* = 5.4 Hz, 1H, bpy), 7.92–8.11 (m, 9H, pyr + bpy), 8.12–8.28 (m, 4H, bpy), 8.36 (d, *J* = 9.3 Hz, 1H, pyr), 8.40–8.52 (m, 4H, bpy), 8.80 (s, 1H, bpy). IR (KBr) *ν* / cm^{-1}: 2930 (m, sh, *ν*($-CH_3$)), 1755 (s, sh, *ν*(C=O)), 1171 (s, sh, *ν*(C–O)). Elemental analyses calcd. (%) for $C_{57}H_{52}Cl_2N_6O_6Ru$•EtOH: C, 62.43; H, 5.15; N, 7.40. Found: C, 62.11; H, 5.30; N, 7.50.

Synthesis of [Re(bpy-pyr)(CO)$_3$(py)]OTf (Complex 6)

The complex was synthesized according to the modification of a literature procedure for the related tricarbonylrhenium(I) bipyridine complexes.[9] $[Re(CO)_5Br]$ (890 mg, 2.19 mmol) and **bpy-pyr** (1 g, 2.4 mmol) were dissolved in toluene (30 mL) and refluxed under N_2 for overnight. After evaporation of the solvent by reduced pressure and purified by column chromatography on silica gel with $CHCl_3$-acetone (10:1 v/v) as the eluent, silver triflate (845 mg, 3.29 mmol) and acetnitrile (50 mL) were added. The mixture was refluxed overnight. After filtration and removal of solvent, the crude product was then mixed with pyridine (194 μL, 2.4 mmol) in THF (50 mL) and was heated to reflux for 4 hours. After the solvent was evaporated under reduced pressure, the product was purified by column chromatography on silica gel with $CHCl_3$-MeOH (4:1 v/v) as the eluent. The product was recrystallized by diffusion of diethyl ether into an acetonitrile solution of the product to afford complex **6** as a yellow solid. Yield: 480 mg (24 %). Positive ESI-MS: ion clusters at m/z 763.8 $[M-OTf]^+$, 684.7

[M–OTf–py]$^{+}$. ^{1}H NMR (300 MHz, CD_3CN, 298 K, relative to Me_4Si, δ / ppm): δ = 2.56 (s, 3H, $–CH_3$), 6.22 (s, 2H, pyr–CH_2O–), 7.36 (d, *J* = 5.4 Hz, 1H, bpy), 7.57 (d, *J* = 6.9 Hz, 2H, py), 8.03–8.30 (m, 12H, pyr+bpy+py), 8.37 (d, *J* = 9.3 Hz, 1H, pyr), 8.60 (s, 1H, py), 8.68 (s, 1H, bpy), 8.88 (d, *J* = 5.4 Hz, 1H, bpy), 9.15 (d, *J* = 5.4 Hz, 1H, bpy). IR (KBr) *v* / cm^{-1}: 2919 (m, sh, *v*($–CH_3$)), 2044, 1915, 1896 (s, sh, *v*(C≡O)), 1750 (s, sh, *v*(C=O)), 1075 (s, sh, *v*(C–O)). Elemental analyses calcd. (%) for $C_{38}H_{25}F_3N_3O_8ReS$: C, 49.24; H, 2.72; N, 4.53. Found: C, 49.35; H, 2.68; N, 4.40.

Preparation of graphene oxide (GO)

The graphite was first pre-oxidized according to a literature procedure reported.[10] The preparation of **GO** was carried out according to the modification of Hummers method.[11] The pre-oxidized graphite powder was put into cold concentrated sulfuric acid (H_2SO_4, 0 ^{o}C, 300 mL). Potassium permanganate ($KMnO_4$, 35 g) was then added gradually and the temperature was kept to be below 20 ^{o}C. The mixture was stirred at 35 ^{o}C for 4 hours, and then diluted with deionized water to about 2 L. Hydrogen peroxide **(**H_2O_2, 30%, 100 mL) was then added dropwise. The mixture was filtered and washed with HCl-H_2O solution (2 L, 1:10 v/v) and deionized water (2 L). The resulting solid was dried. Finally, it was purified by dialysis for one week.

Preparation of reduced graphene oxide (rGO)

The preparation of reduced graphene oxide was carried out according to the modification of a literature method reported by Stankovich and coworkers.[12] The **GO** dispersion (300 mL, 0.2 mg/mL) was sonicated for 1 hour, followed by the addition of hydrazine monohydrate (1.2 mL). The reaction mixture was allowed to stir for 24

hours at 50 ^{o}C. The black hydrophobic powder of reduced graphene oxide was obtained by filtration and was dried in vacuum. The product was well re-dispersed in *N*-methylpyrrolidone (NMP, 300 mL).

Preparation of Ru(II) and Re(I) complex-GO hybrid conjugate (1-GO and 6-GO) via non-covalent functionalization

The non-covalent functionalization of **GO** with ruthenium(II) complex **1** was carried out according to the modification of a literature method.[13] An aqueous solution ruthenium(II) complex **1** (0.01 mM, 100 mL) was prepared and then added to a dispersion of **GO** (100 mL, 0.2 mg/mL). The reaction mixture was allowed to stir overnight at room temperature. After that, the conjugate was purified by repeated centrifugation-redispersion cycles (5000 rpm) and was washed with NMP for the removal of the unattached metal complexes. The non-covalent functionalization of **GO** with rhenium(I) complex (**6-GO**) was carried out with the similar procedures by using rhenium(I) complex **6** instead of ruthenium(II) complex **1**.

Preparation of Ru(II) complex-rGO hybrid conjugate (Ru-rGO) via covalent functionalization

The covalent functionalization of **rGO** with Ru(II) complex was carried out according to the modification of the 1,3-dipolar cycloaddition reported by Guldi and coworkers.[14] The NMP dispersion of **rGO** (11 mg, 20 mL) was re-dispersed in a H_2O-DMF (1:1 v/v) solution of pyr-NMe_3^+ (100 mL, 0.01 mM) and stirred overnight, followed by several centrifugation-redispersion cycles. Sarcosine (48 mg, 0.54 mmol) and 4-carboxybenzaldehyde (230 mg, 1.53 mmol) were then added at 170 ^{o}C and stirred for 7 days. Then, the conjugates were filtered and washed successively with

deionized water, DMF and NMP. The solid product (4 mg) was re-dispersed in DMF (5 mL) and sonicated for 1 hour. It was then added to a solution of $[Ru(bpy)_2(bpy\text{-}CH_2OH)]Cl_2$ (4.1 mg, 0.006 mmol), EDC (1 mg, 0.006 mmol) and HOBt (1 mg, 0.01 mmol) and stirred for 4 days. The crude product was filtered and washed successively with deionized water, DMF and NMP.

Physical Measurements and Instrumentation.

^1H NMR spectra were recorded on a Bruker DPX-300 or Bruker DPX-400 Fourier Transform NMR spectrometer with chemical shifts reported relative to tetramethylsilane, $(CH_3)_4Si$. Positive-ion ESI mass spectra were recorded on Finnigan LCQ mass spectrometer. FTIR spectra of complexes were obtained as KBr disk on a Bio-Rad FTS-7 Fourier transform infrared spectrophotometer (4000–400 cm^{-1}). Elemental analysis of the complexes was performed on a Carlo Erba 1106 elemental analyzer at the Institute of Chemistry of the Chinese Academy of Sciences in Beijing. Electronic absorption spectra were recorded on a Varian Cary 50 UV-vis spectrophotometer. Steady-state excitation and emission spectra were recorded on a Spex Fluorolog-3 Model FL3-211 spectrofluorometer equipped with a R2658P PMT detector. Photophysical measurements in low-temperature glass were carried out with the sample solution loaded in a quartz tube inside a quartz-walled Dewar flask. Liquid nitrogen was placed into the Dewar flask for low temperature (77 K) photophysical measurements. Relative luminescence quantum yields of the ruthenium(II) complexes were measured by the optical dilute method reported by Demas and Crosby.[15] A degassed methanol solution of $[Ru(bpy)_3]Cl_2$ was used as reference (Φ = 0.048, excitation wavelength at 436 nm).[16] Time-resolved emission decay profiles of ruthenium(II) complexes and graphene samples were recorded by with a Horiba Jobin

Yvon FluoroCube based on a time-correlated single-photon counting method, using a nanoLED with peak wavelength and pulse duration equal to 371 nm and < 200 ps, respectively, as the excitation source. For the time-dependent spectroscopic study, diluted porcine liver esterase (10 uL, 0.001 units) was added to the target GO suspension (2.5 mL) in a cuvette with vigorous shaking and the electronic absorption and emission spectra were monitored within 60 minutes and the temperature of the sample was kept at 25 ^{o}C by using thermoelectric peltier. The scanning electron microscopy (SEM) images were recorded on a Hitachi S-4800N Variable Pressure Scanning Electron Microscope operating at 5.0 kV. The samples were prepared by placing a drop (5 μL) of a dilute GO suspension on the surface of a silicon wafer and were then dried in air at room temperature. Transmission electron microscopy (TEM) images, energy-dispersive X-ray (EDX) spectra and electron diffraction images were recorded on a Tecnai 20 (Philips) transmission electron microscope with an accelerating voltage of 200 kV at the Electron Microscope Unit (EMU) of The University of Hong Kong. The samples were prepared by placing a drop (5 μL) of a dilute aqueous suspension of graphene oxide conjugate without addition of buffer on the surface of a 300-mesh copper grid and were then dried in air at room temperature. The accelerating voltage was 120 kV. Thermogravimetric analysis (TGA) thermograms were recorded by Perkin Elmer Thermogravimetric analyzer Pyris 1 TGA equipped with a thermal analysis controller TAC 7/DX. The sample of GO conjugates without the addition of buffer was dried for 3 days under reduced pressure at room temperature before TGA measurement. Raman spectra were recorded with a Raman-Fourier Transform Infra-Red Spectrometer (PE Spectrum 2000) equipped with laser at 1064 nm in the Department of Biology and Chemistry of the City University of Hong Kong. Samples were recorded from the dispersions of the GO conjugates and

the resulted spectra were subtracted from a sample-free solvent background. Topographical images and phase images of atomic force micrographs (AFM) were collected on an Asylem MFP3D atomic force microscope with ARC2 SPM Controller under constant temperature and atmospheric pressure. Samples were prepared by dropcasting diluted solutions onto a silicon wafer. X-Ray diffraction (XRD) experiments were carried out on a Rigaku X-ray diffractometer (D/max 2500 V, using Cu $K\alpha_1$ radiation with a wavelength of 1.5 Å) at 298 K in the State Key Laboratory of Supramolecular Structure and Materials, Jilin University. The samples were prepared in a solid powder form by the drying of a concentrated dispersion.

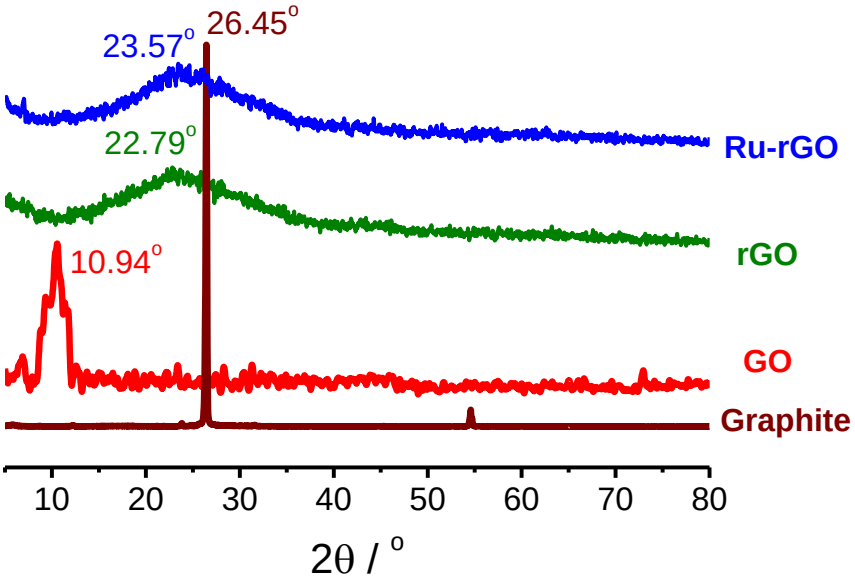

Figure S1. XRD patterns of graphite, **GO**, **rGO** and **Ru-rGO**.

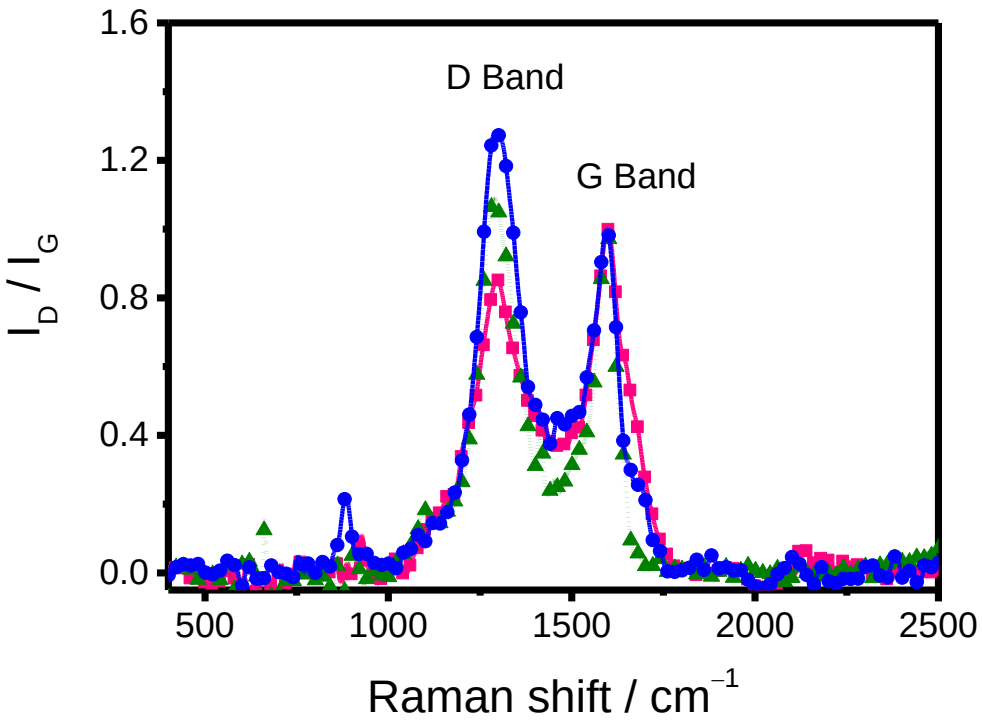

Figure S2. Raman spectra of **GO** (■), **rGO** (▲) and **Ru-rGO** (●). Intensities have been normalized at the G band.

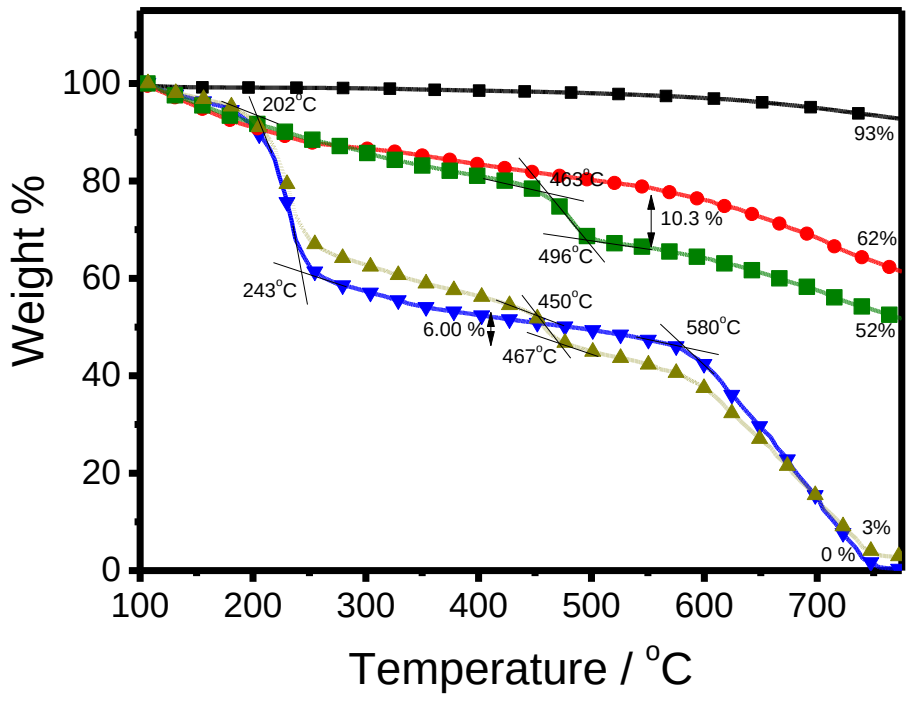

Figure S3. TGA thermograms of graphite flake (■), **GO** (▼), **rGO** (▲), **1-GO** (●) and **Ru-rGO** (■) (scan rate: heating at 10 °C min^{-1}).

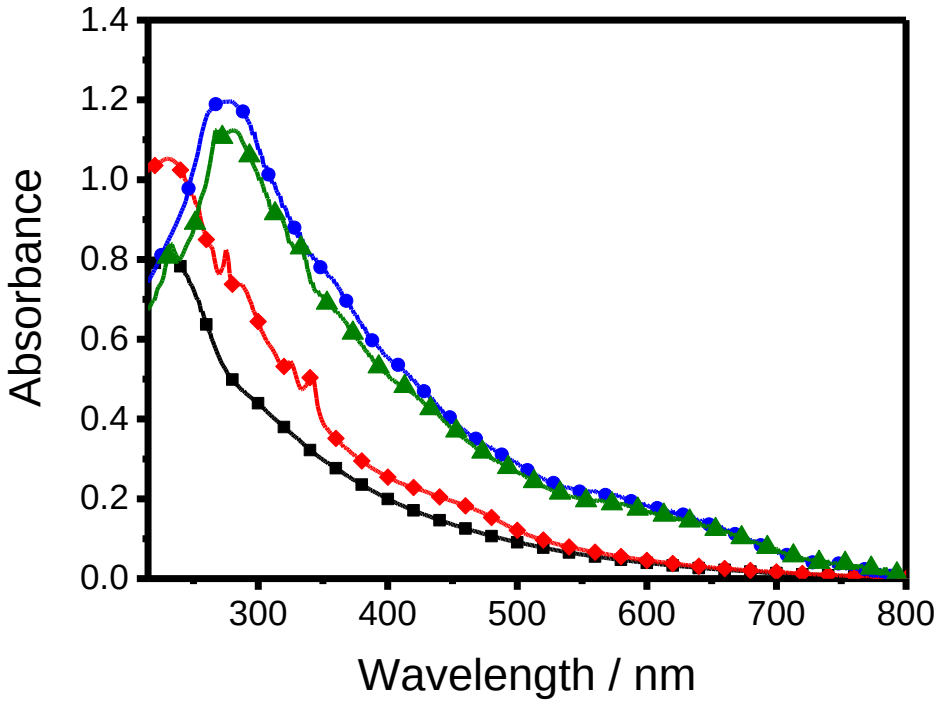

Figure S4. Electronic absorption spectra of **GO** (■), **rGO** (●), **1-GO** (◆) and **Ru-rGO** (▲) in buffer solution at 298 K.

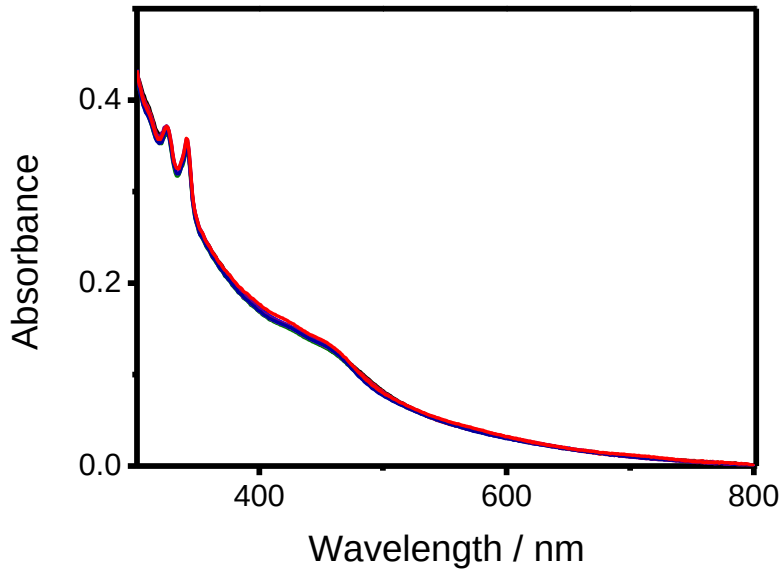

Figure S5. Time-dependent changes in electronic absorption spectra of **1-GO** in buffer solution over 1 hour upon treatment with PLE at 25 ºC.

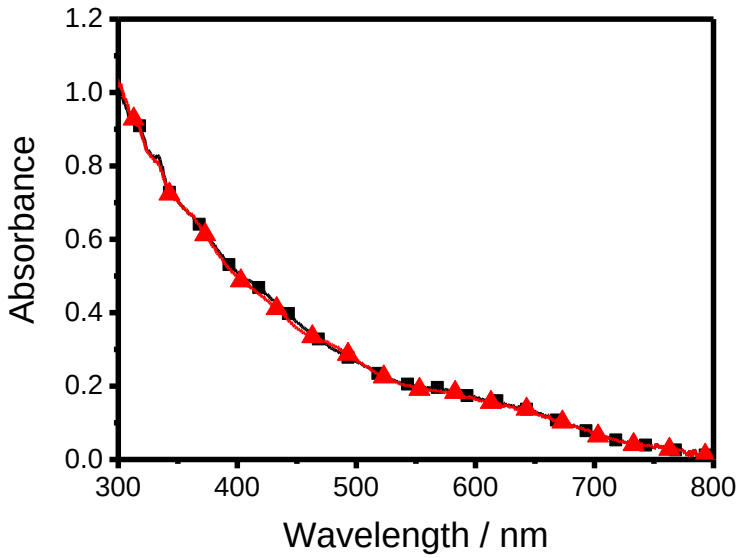

Figure S6. Electronic absorption spectra of **Ru-rGO** in buffer solution before (■) and after (▲) the treatment of PLE at 25 ºC.

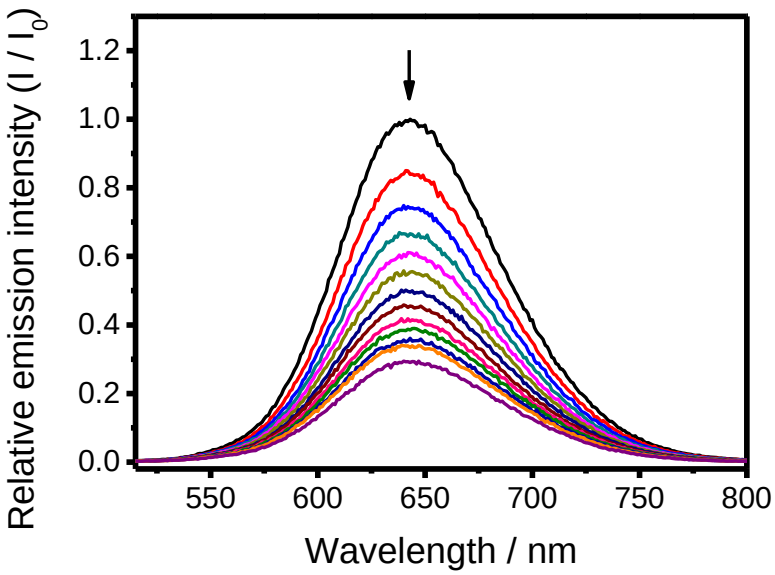

Figure S7. Emission spectral changes upon the repeated addition of 5 μL of GO dispersion (0.2 mg/mL) into an aqueous solution of complex **1** (2 mL, 1.84 x 10^{-5} M).

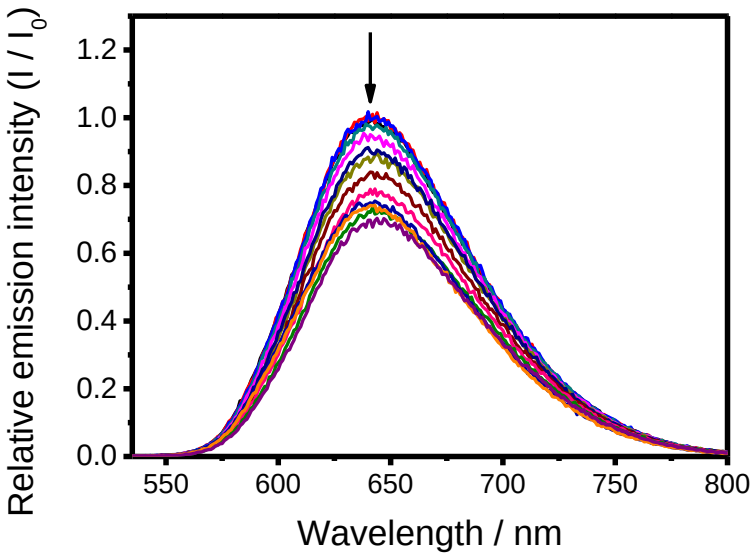

Figure S8. Emission spectral changes upon the repeated addition of 5 μL of GO dispersion (0.2 mg/mL) into an aqueous solution of complex **4** (2 mL, 1.85 x 10^{-5} M).

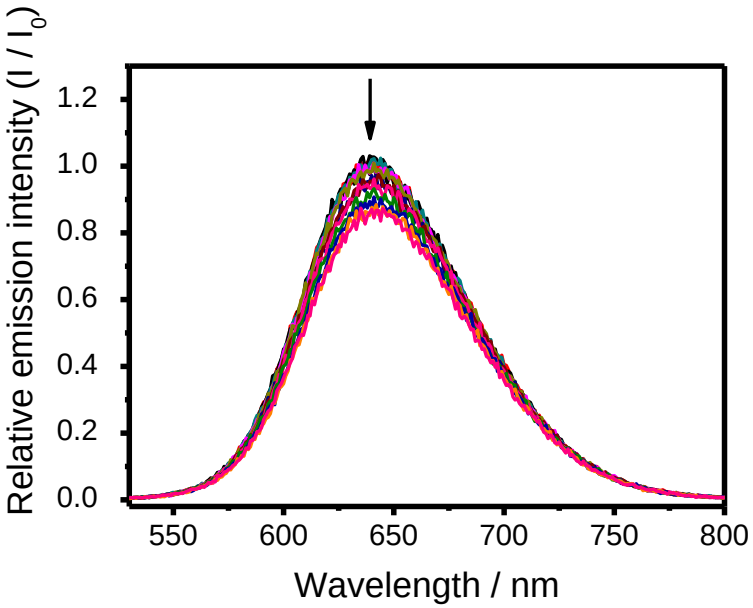

Figure S9. Emission spectral changes upon the repeated addition of 5 μL of GO dispersion (0.2 mg/mL) into an aqueous solution of complex **5** (2 mL, 1.85 x 10^{-5} M).

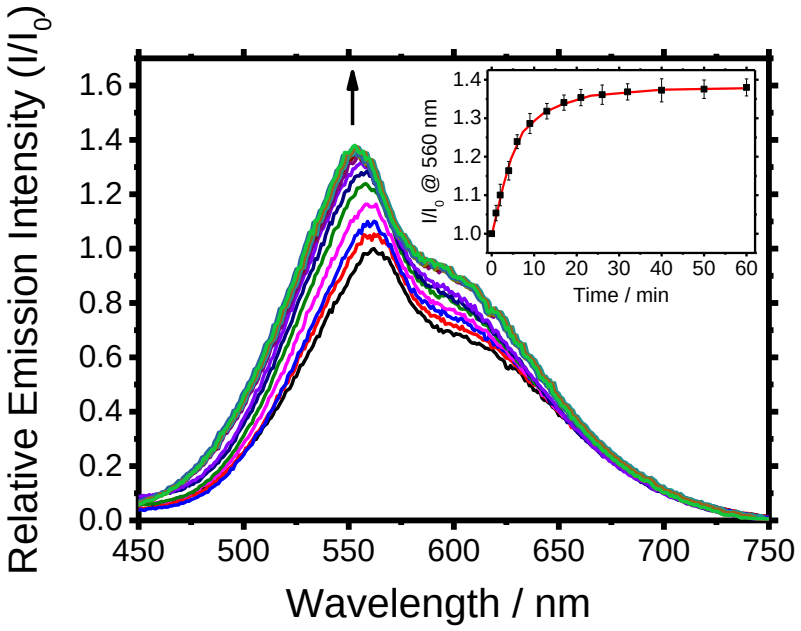

Figure S10. Time-dependent changes in emission spectra of **6-GO** in buffer solution over 1 hour upon treatment with PLE at 25 ºC with excitation wavelength at 340 nm. Inset: A plot of relative emission intensity at 560 nm versus time of esterase treatment.

References

(1) Kikkeri, R.; Liu, X.; Adibekian, A.; Tsai, Y.; Seeberger, P. H. Facile Synthesis of Size Dependent Ru(II)–Carbohydrate Dendrimers via Click Chemistry. *Chem. Commun.* **2010**, *46*, 2197–2199.

(2) Kumari, N.; Dey, N.; Jha, S.; Bhattacharya, S. Ratiometric, Reversible, and Parts per Billion Level Detection of Multiple Toxic Transition Metal Ions Using a Single Probe in Micellar Media. *ACS Appl. Mater. Interfaces* **2013**, *5*, 2438–2445.

(3) Morales, A. F.; Accorsi, G.; Armaroli, N.; Barigelletti, F.; Pope, S. J. A.; Ward, M. D. Interplay of Light Antenna and Excitation "Energy Reservoir" Effects in a Bichromophoric System Based on Ruthenium−Polypyridine and Pyrene Units Linked by a Long and Flexible Poly(ethylene glycol) Chain. *Inorg. Chem.* **2002**, *41*, 6711–6719.

(4) Schulz-Drost, C.; Sgobba, V.; Gerhards, C.; Leubner, S.; Krick Calderon, R. M.; Ruland, A.; Guldi, D. M. Innovative Inorganic–Organic Nanohybrid Materials: Coupling Quantum Dots to Carbon Nanotubes. *Angew. Chem. Int. Ed.* **2010**, *49*, 6425–6429.

(5) Sullivan, B. P.; Salmon, D. J.; Meyer, T. J. Mixed Phosphine 2,2'-Bipyridine Complexes of Ruthenium. *Inorg. Chem.* **1978**, *17*, 3334–3341.

(6) Schmidt, S. P.; Trogler, W. C.; Fred, B. Pentacarbonylrhenium Halides. *Inorg. Synth.* **1990**, *28*, 154–159.

(7) Haddour, N.; Chauvin, J.; Gondran, C.; Cosnier, S. Photoelectrochemical Immunosensor for Label-Free Detection and Quantification of Anti-cholera Toxin Antibody. *J. Am. Chem. Soc.* **2006**, *128*, 9693–9698.

(8) Wrighton, M. S.; Morse, D. L. Nature of the Lowest Excited State in

Tricarbonylchloro-1,10-phenanthrolinerhenium(I) and Related Complexes. *J. Am. Chem. Soc.* **1974**, *96*, 998–1003.

(9) Leung, F. C.-M.; Tam, A. Y.-Y.; Au, V. K.-M.; Li, M.; Yam, V. W.-W. Förster resonance energy transfer studies of luminescent gold nanoparticles functionalized with ruthenium(II) and rhenium(I) complexes: modulation via esterase hydrolysis. *ACS Appl. Mater. Interfaces* **2014**, *6*, 6644–6653.

(10) Tang, L.; Wang, Y.; Li, Y.; Feng, H.; Lu, J.; Li, J. Preparation, Structure, and Electrochemical Properties of Reduced Graphene Sheet Films. *Adv. Funct. Mater.* **2009**, *19*, 2782–2789.

(11) Hummers, W. S.; Offeman, R. E. Preparation of Graphitic Oxide. *J. Am. Chem. Soc.* **1958**, *80*, 1339–1339.

(12) Stankovich, S.; Piner, R. D.; Chen, X.; Wu, N.; Nguyen, S. T.; Ruoff, R. S. Stable Aqueous Dispersions of Graphitic Nanoplatelets via the Reduction of Exfoliated Graphite Oxide in the Presence of Poly(sodium 4-styrenesulfonate). *J. Mater. Chem.* **2006**, *16*, 155–158.

(13) Chen, Q.; Wei, W.; Lin, J. Homogeneous Detection of Concanavalin A Using Pyrene-Conjugated Maltose Assembled Graphene Based on Fluorescence Resonance Energy Transfer. *Biosens. Bioelectron.* **2011**, *26*, 4497–4502.

(14) Ragoussi, M.; Malig, J.; Katsukis, G.; Butz, B.; Spiecker, E.; de la Torre, G.; Torres, T.; Guldi, D. M. Linking Photo- and Redoxactive Phthalocyanines Covalently to Graphene. *Angew. Chem. Int. Ed.* **2012**, *51*, 6421–6425.

(15) Crosby, G. A.; Demas, J. N. Measurement of Photoluminescence Quantum Yields. Review *J. Phys. Chem.* **1971**, *75*, 991–1024.

(16) Nakamaru, K. Solvent Effect on the Nonradiative Deactivation of the Excited State of Tris(2,2’-bipyridyl)ruthenium(II) Ion. *Bull Chem. Soc. Jpn.* **1982**, *55*,

1639–1640.